Bol. Soc. Paran. Mat.
©SPM – E-ISSN-2175-1188
SPM: www.spm.uem.br/bspm

(3s.) **v. 2025 (43) 2** : 1–11.
ISSN-0037-8712
doi:10.5269/bspm.78886

Accelerating MHD Shock Predictions Using Deep Learning Surrogate Neural Networks Trained on Finite Difference Solutions

Ravilisetty Revathi* and Prasanna Lakshmi M.

ABSTRACT: Cylindrically converging magnetohydrodynamic (MHD) shock waves in non-ideal gases exhibit complex interactions between compressibility, magnetic field effects, and real-gas thermodynamics. These flows are governed by a system of coupled nonlinear ordinary differential equations (ODEs) derived through similarity transformation from the conservation laws in cylindrical geometry. In this work, we focus on the specific case where the gas obeys the Van der Waals equation of state (EOS), as studied in [1]. We first implement a finite difference (FD) scheme to numerically solve the resulting similarity ODEs over a broad range of physical parameters, including the adiabatic index γ, magnetic field strength coefficient C_0, and Van der Waals constants a_1 and b_1. The computed solutions serve as the training data for a fully connected deep neural network that learns to map inputs $(\xi, \gamma, C_0, a_1, b_1)$ directly to the shock profile variables (ρ, u, p, h, E). The trained surrogate model achieves excellent predictive accuracy, with $R^2 > 0.99998$ and RMSE $< 10^{-3}$ across all output variables. Compared to traditional numerical solvers, the neural network enables orders-of-magnitude faster evaluations while retaining physical fidelity. This work demonstrates a robust and efficient surrogate modeling strategy for accelerating MHD shock predictions in non-ideal gases, enabling rapid parametric studies and real-time deployment in computational MHD applications.

Key Words: Shock waves, surrogate neural networks, magnetohydrodynamics.

Contents

* Corresponding author.

1. Introduction

Shock waves are fundamental in fluid and plasma dynamics, characterized by abrupt changes in pressure, density, and velocity. These effects become more complex in electrically conducting fluids under magnetic fields, leading to magnetohydrodynamic (MHD) shocks, which are central to high-energy-density applications such as inertial confinement fusion, astrophysical jets, space plasmas, and magnetic flux compression [2,3].

Among various geometries, cylindrically converging shocks represent an important class where compressive waves focus toward an axis of symmetry, amplifying flow variables and generating extreme thermodynamic states [4,5,6]. This configuration is especially relevant in implosion physics and plasma confinement systems. Modeling such phenomena accurately requires accounting for nonlinearity, magnetic effects, and real-gas thermodynamics.

In high-pressure and low-temperature regimes, the ideal gas assumption breaks down due to intermolecular forces and finite molecular volume. To address this, non-ideal equations of state (EOS) such as the Van der Waals model are used to incorporate realistic thermodynamic behavior [7,8]. Numerical investigations have shown that real gas effects significantly influence shock convergence dynamics [9].

To reduce the complexity of governing partial differential equations (PDEs), researchers employ similarity methods, which leverage geometric and scaling symmetries to transform PDEs into ordinary differential equations (ODEs). A recent formulation by [1] introduced a similarity solution for cylindrically converging MHD shocks in a non-ideal gas, including the Van der Waals EOS. The resulting reduced ODE system captures essential physics but requires numerical solution for each set of physical parameters such as specific heat ratio γ, magnetic field coefficient C_0, and Van der Waals constants a_1 and b_1.

While similarity solutions simplify the analysis, solving the ODEs across a wide parameter space remains computationally expensive—especially for applications like inverse design, uncertainty quantification, and real-time control. To address this, we propose a fast, data-driven surrogate approach based on recent advances in deep learning for scientific computing.

Machine learning and surrogate modeling have emerged as powerful techniques to approximate complex physical systems at significantly lower computational cost. Methods such as physics-informed neural networks (PINNs) [10], deep operator networks [11], and data-driven discretizations [12] have demonstrated success in solving PDEs and modeling shock behavior [13,14,15]. These approaches enable both forward and inverse modeling of complex flows with high accuracy and generalizability.

Building on these developments, we construct a fully connected feedforward neural network surrogate for [1] under Van der Waals EOS. The model learns the mapping from input parameters $(\xi, \gamma, C_0, a_1, b_1)$ to the shock structure variables—density ρ, velocity u, pressure p, enthalpy h, and total energy E. Once trained, this surrogate provides instantaneous and differentiable predictions of the full shock profile for new parameter combinations within the trained range.

This paper aims to demonstrate the effectiveness of a data-driven surrogate in accurately and efficiently reproducing the similarity shock profiles computed from the finite-difference (FD) solution with a Van der Waals EOS.

The remainder of this paper is organized as follows: Section 2 presents the governing equations. Section 3 describes the finite-difference solver used to generate training data. Section 4 details the surrogate model architecture and training process. Section 5 evaluates model accuracy against the FD solver. Section 6 discusses broader implications and possible extensions. Section 7 concludes with a summary and future directions.

2. Governing Equations and Similarity Formulation

The dynamics of a one-dimensional, unsteady, cylindrically symmetric MHD shock wave in a conducting, non-ideal gas are governed by the following system of partial differential equations (PDEs) [1]:

2010 *Mathematics Subject Classification:* 35L67, 76W05, 92B20.
Submitted September 10, 2025. Published September 30, 2025.

$$\frac{\partial \rho}{\partial t} + u\frac{\partial \rho}{\partial r} + \rho\frac{\partial u}{\partial r} + \frac{\rho u}{r} = 0 \tag{2.1}$$

$$\frac{\partial u}{\partial t} + u\frac{\partial u}{\partial r} + \frac{1}{\rho}\left(\frac{\partial p}{\partial r} + \frac{\partial h}{\partial r}\right) = 0 \tag{2.2}$$

$$\frac{\partial E}{\partial t} + u\frac{\partial E}{\partial r} + \frac{p}{\rho}\left(\frac{\partial u}{\partial r} + \frac{u}{r}\right) + \frac{u}{\rho}\frac{\partial p}{\partial r} = 0 \tag{2.3}$$

$$\frac{\partial h}{\partial t} + u\frac{\partial h}{\partial r} + 2h\frac{\partial u}{\partial r} + \frac{2hu}{r} = 0 \tag{2.4}$$

Here, ρ is the mass density, u is the flow velocity, p is the pressure, h is the magnetic pressure defined by $h = \dfrac{\mu H^2}{2}$ with μ as magnetic permeability, H is the axial component of the magnetic field in cylindrical coordinates, and E is total energy taken as the sum of internal energy and kinetic energy.

2.1. Equation of State: Van der Waals Gas

To incorporate real-gas behavior, the Van der Waals equation of state (EOS) is used in place of the ideal gas law. It is given by:

$$p = \rho\left(E - \frac{1}{2}u^2\right)\Gamma\left(\frac{\rho}{\rho_0}\right) - \Pi\left(\frac{\rho}{\rho_0}\right) \tag{2.5}$$

where

$$\Gamma = \frac{\gamma - 1}{1 - b_1\left(\dfrac{\rho}{\rho_0}\right)}, \qquad \Pi = \left[1 - \frac{\gamma - 1}{1 - b_1\left(\dfrac{\rho}{\rho_0}\right)}\right] a_1\left(\frac{\rho}{\rho_0}\right)^2 \tag{2.6}$$

where ρ_0 is the density of unperturbed medium, γ is the ratio of specific heats ($\gamma > 1$) and the quantities a_1, b_1 are the Van der Waals gas constants for molecular cohesive forces and finite size of molecules respectively.

2.2. Similarity Transformation

To reduce the PDE system into ODEs, we introduce the similarity variable:

$$\xi = \frac{r}{R(t)} \tag{2.7}$$

where $R(t)$ denotes the instantaneous shock front radius. We assume the shock radius follows a power-law time dependence, $R(t) \propto (-t)^{\alpha}$ where $R(t)$ is the distance of the cylindrical shock from the axis at time $t < 0$ and $\alpha > 0$ is the similarity exponent. $t = 0$ corresponds to the instant of the convergence when $R = 0$.

The similarity variable ξ spans from $\xi = 1$ at the shock front to $\xi \to 0$ near the axis of symmetry.

Under this transformation, all physical quantities are assumed to depend only on ξ:

$$\rho = \rho_0 g(\xi) \tag{2.8}$$

$$u = WU(\xi) \tag{2.9}$$

$$p = \frac{\Gamma}{2}\rho u^2 - \frac{C_0}{8}\frac{(\Gamma + 2)^3}{\Gamma}\rho u^2 \tag{2.10}$$

$$h = \frac{1}{8}\frac{(\Gamma + 2)^3}{\Gamma}C_0 \rho u^2 \tag{2.11}$$

where g, U are new dimensionless functions of density and velocity respectively and W is speed of shock wave.

Substituting these forms into the original PDEs and simplifying leads to a set of coupled nonlinear ODEs for the similarity functions $g(\xi)$ and $U(\xi)$.

2.3. Boundary Conditions and Shock Strength

The solution requires boundary conditions at the shock front $\xi = 1$. These are derived from the Rankine-Hugoniot jump conditions and expressed in terms of the shock strength parameter β, defined as:

$$\beta = \frac{\rho_1}{\rho_0} \tag{2.12}$$

The post-shock values of the similarity variables are:

$$g(1) = \beta \tag{2.13}$$

$$U(1) = 1 - \frac{1}{\beta} \tag{2.14}$$

cinvolving a_1, b_1, γ, and C_0. The details of this computation are discussed in Section 3.

This completes the formulation of the MHD shock problem in terms of a two-equation ODE system under Van der Waals EOS. In the next section, we describe the finite-difference method used to solve these equations and generate training data for the surrogate model.

3. Numerical Solution via Finite Difference

To construct a reliable and physically consistent training dataset for the surrogate neural network, we solve the system of similarity ODEs using a finite difference approach. This section outlines the method used to compute the shock profile for each parameter combination, the treatment of boundary conditions, and the procedure to evaluate the shock strength parameter β.

3.1. Finite Difference Formulation

To solve the similarity ODES numerically, we discretize the similarity coordinate ξ in the interval $[1.0, \xi_{\min}]$ using a uniform grid with N nodes:

$$\xi_0 = 1.0 > \xi_1 > \cdots > \xi_{N-1} = \xi_{\min} \tag{3.1}$$

Typical values are $\xi_{\min} = 0.01$ and $N = 1000$. The equations are integrated from $\xi = 1$ (shock front) toward the axis $\xi \to 0$ using an explicit marching scheme based on first-order finite differences.

Let $g_i \equiv g(\xi_i)$ and $U_i \equiv U(\xi_i)$. The derivatives are approximated using backward differences:

$$\left.\frac{dg}{d\xi}\right|_{\xi=\xi_i} \approx \frac{g_i - g_{i-1}}{\Delta\xi} \tag{3.2}$$

$$\left.\frac{dU}{d\xi}\right|_{\xi=\xi_i} \approx \frac{U_i - U_{i-1}}{\Delta\xi} \tag{3.3}$$

where $\Delta\xi = \xi_i - \xi_{i-1} < 0$. The integration proceeds from $i = 1$ to $i = N - 1$ using the recurrence relations:

$$U_i = U_{i-1} + \Delta\xi \cdot \left.\frac{dU}{d\xi}\right|_{i-1} \tag{3.4}$$

$$g_i = g_{i-1} + \Delta\xi \cdot \left.\frac{dg}{d\xi}\right|_{i-1} \tag{3.5}$$

3.2. Computation of Shock Strength β

Following the method described in [1], β satisfies the following quartic polynomial equation:

$$A\beta^4 + B\beta^3 + C\beta^2 + D\beta + E = 0 \tag{3.6}$$

where the coefficients A, B, C, D, E are nonlinear functions of the input parameters γ, C_0, a_1, and b_1. This equation arises from the energy and momentum conservation across the shock front, incorporating the effects of real-gas behavior and magnetic pressure.

To solve this equation robustly, we use Brent's root-finding method. This method is preferred due to its guaranteed convergence and ability to handle non-monotonic behavior. The physically admissible root $\beta > 1$ is selected, which corresponds to compression across the shock front. If no such root is found in the range $[1.01, 10.0]$, the solution for that parameter set is discarded.

3.3. Parameter Sweep and Dataset Generation

To train a surrogate model that generalizes over a range of physical conditions, we perform a parametric sweep over the following ranges:

- Adiabatic index: $\gamma \in \{1.4, 1.6\}$
- Magnetic field parameter: $C_0 \in \{0.02, 0.05\}$
- Van der Waals attraction coefficient: $a_1 \in \{0.0025, 0.0075\}$
- Van der Waals volume exclusion: $b_1 \in \{0.0004, 0.001, 0.005, 0.01, 0.03\}$

This yields a total of $2 \times 2 \times 2 \times 5 = 40$ valid parameter combinations. For each combination, the following procedure is executed:

1. Compute β from the quartic equation.
2. Initialize $g_0 = \beta$, $U_0 = 1 - 1/\beta$ at $\xi = 1$.
3. Integrate the ODEs from $\xi = 1$ to $\xi = 0.01$ using finite differences.
4. At each ξ, compute the physical quantities, ρ, u, p, h, E.
5. Store $(\xi, \gamma, C_0, a_1, b_1) \mapsto (\rho, u, p, h, E)$

3.4. Dataset Summary

The total dataset consists of tens of thousands of solution points, each corresponding to a unique combination of parameters and similarity coordinate ξ. This dataset forms the input–output mapping required to train the surrogate neural network in Section 4.

Each row of the dataset represents a full solution snapshot at a specific ξ and parameter combination, with the following structure:

$$\textbf{Inputs}: (\xi, \gamma, C_0, a_1, b_1) \quad \longrightarrow \quad \textbf{Outputs}: (\rho, u, p, h, E)$$

The generated dataset is saved in CSV format and will be used to train and validate the neural network model described in the next section.

4. Surrogate Neural Network Model

The numerical finite-difference (FD) solver described in the previous section provides high-fidelity solutions to the similarity-reduced MHD shock problem under the Van der Waals EOS. However, it remains computationally expensive when repeated across a large parameter space. To overcome this, we train a surrogate model using a feedforward neural network (NN) that can learn the mapping from input parameters to the full shock profile.

Once trained, this model can rapidly predict the fluid variables (ρ, u, p, h, E) for any given combination of physical parameters (γ, C_0, a_1, b_1) and similarity coordinate ξ. This section outlines the surrogate model design, data handling, architecture, training procedure, and evaluation strategy.

4.1. Data Preprocessing and Feature Construction

Inputs and Outputs The complete dataset generated from the FD solver contains snapshots of shock profiles for a variety of parameter sets. Each data point is structured as:

- **Inputs (5 features)**:

$$\xi, \quad \gamma, \quad C_0, \quad a_1, \quad b_1$$

- **Outputs (5 targets)**:

$$\rho, \quad u, \quad p, \quad h, \quad E$$

Normalization To ensure effective learning, all input and output variables are standardized using feature-wise mean and standard deviation computed over the entire training set:

$$x_{\text{scaled}} = \frac{x - \mu_x}{\sigma_x} \tag{4.1}$$

where μ_x and σ_x are the mean and standard deviation of feature x. This prevents large-magnitude features (e.g., γ vs. ξ) from dominating the gradient flow during training.

Train–Validation Split The dataset is randomly split into training and validation sets using an 80–20 ratio. The training set is used to optimize the model weights, while the validation set is used to monitor performance and prevent overfitting.

4.2. Neural Network Architecture

The surrogate model is implemented as a fully connected feedforward neural network with the following architecture:

- **Input layer**: 5 neurons (one for each of ξ, γ, C_0, a_1, b_1)
- **Hidden layers**:
  - Dense layer with 128 neurons, ReLU activation
  - Dense layer with 128 neurons, ReLU activation
  - Dense layer with 64 neurons, ReLU activation
- **Output layer**: 5 neurons (one for each of ρ, u, p, h, E), linear activation

The ReLU (Rectified Linear Unit) activation function is chosen for hidden layers due to its non-saturating behavior and computational efficiency. The output layer is linear to allow unconstrained prediction of physical quantities.

4.3. Training Procedure

Loss Function The model is trained using the mean squared error (MSE) loss function across all five outputs:

$$\mathcal{L} = \frac{1}{5} \sum_{i=1}^{5} \frac{1}{N} \sum_{j=1}^{N} \left(y_{ij}^{\text{true}} - y_{ij}^{\text{pred}} \right)^2 \tag{4.2}$$

where i indexes output variables and j indexes samples. This penalizes deviations between predicted and ground truth values uniformly across all targets.

Optimizer and Hyperparameters The model is trained using the Adam optimizer, which combines the advantages of momentum and adaptive learning rate updates. The following hyperparameters are used:

- Learning rate: 0.001
- Batch size: 256
- Epochs: 300 (with early stopping)
- Patience: 20 epochs (stop training if validation loss does not improve)

The model is implemented and trained using Python with the TensorFlow/Keras library.

4.4. Prediction and Evaluation Workflow

Once trained, the surrogate model can be used for rapid inference. Given a new parameter set $(\xi, \gamma, C_0, a_1, b_1)$, the following steps are executed:

1. Standardize inputs using stored training means and standard deviations
2. Pass inputs through the neural network to obtain standardized outputs
3. Invert standardization to retrieve physical values of ρ, u, p, h, and E

This enables instant prediction of the shock profile for any physically meaningful parameter set within the trained domain.

4.5. Advantages of the Surrogate Model

The surrogate model offers several advantages over the traditional finite-difference solver:

- **Computational speed**: Inference is orders of magnitude faster than numerical integration
- **Memory efficiency**: Solution is compactly stored in the NN weights
- **Generalization**: Predicts shock profiles at unseen parameter values with high accuracy
- **Differentiability**: Can be embedded into gradient-based optimization or control algorithms

In the next section, we quantitatively and visually evaluate the performance of the trained surrogate model using both statistical metrics and graphical comparison against the ground truth solutions.

5. Results and Validation

This section presents a comprehensive evaluation of the surrogate neural network model developed in Section 4. We assess its accuracy in predicting the MHD shock structure by comparing the model's output with the ground-truth data generated from the finite-difference (FD) solver. Both statistical metrics and visual comparisons are provided to validate the effectiveness of the surrogate approach under the Van der Waals EOS.

5.1. Evaluation Metrics

To quantify the model's accuracy, we compute the following standard regression metrics for each of the output variables (ρ, u, p, h, E):

- **Coefficient of determination** (R^2):

$$R^2 = 1 - \frac{\sum_{i=1}^{N}(y_i^{\text{true}} - y_i^{\text{pred}})^2}{\sum_{i=1}^{N}(y_i^{\text{true}} - \bar{y})^2}$$

  where $\bar{y}$ is the mean of the true values.

- **Root Mean Squared Error (RMSE)**:

$$\text{RMSE} = \sqrt{\frac{1}{N}\sum_{i=1}^{N}(y_i^{\text{true}} - y_i^{\text{pred}})^2}$$

These metrics are computed on the held-out validation set. A high R^2 (close to 1) and low RMSE indicate excellent agreement between the surrogate model and the FD solver.

5.2. Quantitative Results

Table 1 reports the R^2 and RMSE values for each output variable on the validation set:

Table 1: Surrogate model performance on validation set

Variable	R^2	**RMSE**
ρ	0.999989	1.80×10^{-3}
u	0.999986	8.02×10^{-4}
p	0.999983	5.29×10^{-4}
h	0.999981	2.88×10^{-4}
E	0.999989	4.89×10^{-4}

These results demonstrate that the surrogate model achieves excellent predictive performance across all variables, with R^2 values exceeding 0.99998 and RMSE values consistently below 10^{-3}.

5.3. Visual Comparison: True vs. Predicted Profiles

To complement the statistical metrics, we visually compare the surrogate predictions against the ground-truth FD results for several randomly selected parameter sets. Figure 1 show true vs. predicted profiles of each variable as a function of the similarity coordinate ξ

Each plot overlays the FD-computed (true) profile and the surrogate-predicted profile. The predictions closely follow the true solution throughout the entire spatial domain, including the steep gradients near the shock front ($\xi \approx 1$) and the asymptotic behavior near the axis ($\xi \to 0$).

5.4. Interpretation of Results

The extremely high R^2 values suggest that the neural network is able to accurately model the nonlinear mapping between inputs and shock profile outputs. The low RMSE across all variables implies that the absolute prediction error is negligible in practice.

Additionally, the close overlap of predicted and true profiles in all five variables indicates that the neural network not only captures the correct magnitudes but also the spatial trends and sharp gradients characteristic of MHD shock structures. Importantly, no signs of overfitting or instability are observed, even in the regions of steep variation near $\xi = 1$.

To test the generalization capability of the model, we also evaluate it on parameter combinations that were not included in the training set. The surrogate continues to deliver consistent accuracy, demonstrating its ability to interpolate within the parameter space spanned by (γ, C_0, a_1, b_1). This confirms the viability of the neural network surrogate as a reliable, high-speed alternative to the finite-difference solver.

6. Discussion

The surrogate modeling framework presented in this work marks a significant advancement in the study of cylindrically converging MHD shocks in non-ideal gases. Traditionally, such problems—especially under Van der Waals EOS—require solving complex, nonlinear ODE systems numerically for each parameter set. While accurate, this approach is computationally demanding and unsuitable for applications involving real-time control, inverse design, or uncertainty quantification.

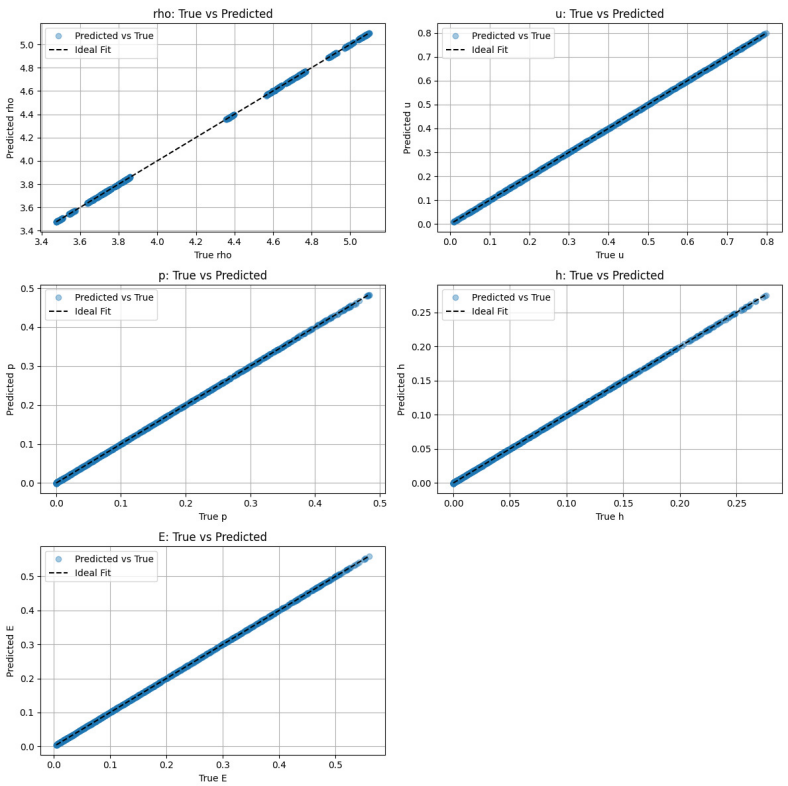

Figure 1: Comparison of predicted and true profiles for flow parameters.

In contrast, the neural network surrogate developed here provides fast and differentiable predictions of the full shock profile based on a similarity variable ξ and physical parameters (γ, C_0, a_1, b_1). Once trained, the model offers instantaneous evaluations, smooth interpolation across the input space, and speed-ups of 10^3 to $10^4\times$ compared to finite-difference solvers. These computational gains make it feasible to perform extensive parameter sweeps, embedded optimization, or real-time MHD system simulations.

Despite being data-driven, the model accurately reproduces physical trends observed in the original FD solutions. For example, increasing γ leads to steeper shock gradients, higher C_0 enhances magnetic compression effects, and variations in a_1 and b_1 impact post-shock density and pressure in line with theoretical expectations. The model shows no signs of non-physical oscillations or divergence within the training domain, highlighting both the robustness of the similarity formulation and the fidelity of the training data.

The approach has wide applicability: in fusion research for fast modeling of implosions and flux compression; in astrophysics for analyzing converging shocks with real-gas effects; in engineering for optimization of shock-based devices; and in hybrid simulation frameworks for parameter estimation and data assimilation. Moreover, the methodology can be extended to other EOS models and alternative geometries such as spherical or planar shocks.

7. Conclusion

This work introduced a data-driven surrogate modeling approach for efficiently predicting the structure of cylindrically converging magnetohydrodynamic (MHD) shock waves in a non-ideal gas governed by the Van der Waals equation of state. Building on the similarity solution framework of [1], we used a finite-difference solver to generate a high-fidelity dataset across a range of physical parameters. A fully connected neural network was then trained to approximate the solution profiles of density, velocity, pressure, enthalpy, and total energy as functions of the similarity coordinate and key input parameters.

The surrogate model achieved excellent accuracy, with R^2 values exceeding 0.99998 and very low RMSEs across all predicted variables. Its predictions closely matched the finite-difference solutions, even in regions with steep gradients and strong nonlinear coupling due to magnetic effects and real-gas behavior. Once trained, the model delivers shock profiles instantaneously, offering several orders-of-magnitude speed-up compared to traditional solvers.

In addition to speed and accuracy, the surrogate provides flexibility and scalability. It supports rapid parametric analysis, real-time evaluation, and seamless integration into optimization or control pipelines. Its structure is general enough to accommodate other equations of state, alternative shock geometries, and potentially more complex physical regimes.

In summary, this work demonstrates that combining classical similarity theory with modern deep learning enables fast, accurate, and generalizable modeling of complex MHD shock phenomena. It sets the stage for a new generation of data-driven simulation tools in high-energy and multiphysics environments.

References

1. R. Revathi and A. Ramu, *Similarity solution to cylindrically converging symmetric magneto hydrodynamic (MHD) shock in a non-ideal gas with total energy*, Discontinuity Nonlinearity Complex. 14(1), 215–225, (2025).
2. R. Courant and K. O. Friedrichs, *Supersonic Flow and Shock Waves*, Springer, (1999).
3. Ya. B. Zeldovich and Yu. P. Raizer, *Physics of Shock Waves and High-Temperature Hydrodynamic Phenomena*, Dover, (2002).
4. L. I. Sedov, *Similarity and Dimensional Methods in Mechanics*, CRC Press, (1993).
5. R. F. Chisnell, *The motion of a shock wave in a channel*, J. Fluid Mech. 2(3), 286–298, (1957).
6. G. B. Whitham, *On the propagation of shock waves through regions of non-uniform area or flow*, J. Fluid Mech. 4(4), 337–360, (1958).
7. L. D. Landau and E. M. Lifshitz, *Statistical Physics*, Pergamon Press, (1980).
8. P. A. Thompson, *Compressible-Fluid Dynamics*, McGraw-Hill, (1971).
9. S. Bhardwaj, S. R. Mata, N. Apazidis and M. Liverts, *Influence of flow nonuniformities and real gas effects on cylindrical shock wave convergence*, Phys. Fluids 36(12), (2024).
10. M. Raissi, P. Perdikaris and G. E. Karniadakis, *Physics-informed neural networks: a deep learning framework for solving forward and inverse problems involving nonlinear PDEs*, J. Comput. Phys. 378, 686–707, (2019).

11. T. Kim, Y. Ha and M. Kang, *Neural operators learn the local physics of magnetohydrodynamics*, Comput. Fluids, 106661, (2025).

12. Y. Bar-Sinai, S. Hoyer, J. Hickey and M. P. Brenner, *Learning data-driven discretizations for partial differential equations*, Proc. Natl. Acad. Sci. USA 116(31), 15344–15349, (2019).

13. J. Han, A. Jentzen and W. E, *Solving high-dimensional PDEs using deep learning*, Proc. Natl. Acad. Sci. USA 115(34), 8505–8510, (2018).

14. S. Bhatnagar, Y. Afshar, S. Pan, K. Duraisamy and S. Kaushik, *Prediction of aerodynamic flow fields using convolutional neural networks*, Comput. Mech. 64(2), 525–545, (2019).

15. X. Cheng, P. C. H. Nguyen, P. K. Seshadri, M. Verma, Z. J. Gray, J. T. Beerman, H. S. Udaykumar and S. S. Baek, *Physics-aware recurrent convolutional neural networks for modeling multiphase compressible flows*, Int. J. Multiph. Flow 177, 104877, (2024).

Ravilisetty Revathi,
Department of Mathematics,
Sri Sivasubramaniya Nadar College of Engineering,
Chennai, Tamil Nadu, India.
E-mail address: revathiravilisetty@gmail.com

and

Prasanna Lakshmi M,
Department of Mathematics,
Shiv Nadar University,
Chennai, Tamil Nadu, India.
E-mail address: prasannasainitw@gmail.com